

NASA TECHNICAL MEMORANDUM

NASA TM X-62,391

NASA TM X-62,391

(NASA-TM-X-62391)	MEASUREMENTS OF THE	N75-12896
VORTEX WAKES OF A SUBSONIC AND		
SUPERSONIC TRANSPORT MODEL IN THE 40 BY		
80 FOOT WIND TUNNEL (NASA) 19 p HC		Unclas
\$3.25	CSSL 01B G3/02	03678

MEASUREMENTS OF THE VORTEX WAKES OF A SUBSONIC- AND A SUPERSONIC-TRANSPORT MODEL IN THE 40- BY 80-FOOT WIND TUNNEL

V. J. Rossow and V. R. Corsiglia

Ames Research Center
Moffett Field, Calif. 94035

and

J. J. Phillippe

ONERA
Chatillon, France



September 1974

NOMENCLATURE

A	aspect ratio, b^2/S
b	span of wing
c	wing chord
C_z	rolling-moment coefficient, torque/ $(\frac{1}{2} \rho U_\infty^2 S b)$
C_L	lift-coefficient, lift/ $(\frac{1}{2} \rho U_\infty^2 S)$
S	wing area
x, y, z	coordinate axes; x is streamwise and z is vertical
U_∞	free-stream velocity (alined with x axis)
α	angle of attack
Γ	circulation
ρ	air density

Subscripts

f	following model that encounters wake
g	model that generates wake
∞	free stream

MEASUREMENTS OF THE VORTEX WAKES OF A SUBSONIC- AND A
SUPERSONIC-TRANSPORT MODEL IN THE
40- BY 80-FOOT WIND TUNNEL

V. J. Rossow and V. R. Corsiglia
Ames Research Center

and

J. J. Phillippe
ONERA, Chatillon, France

SUMMARY

The rolling moment induced on aircraft models in the wake of a model of a subsonic transport and of a supersonic transport was measured as a function of angle of attack for several configurations. A description of the tests and a presentation and analysis of the data is given in this memorandum.

INTRODUCTION

The trend toward higher air traffic density at airports coupled with the increasing differences in the size of aircraft enhances the hazard to small aircraft that might encounter a large aircraft wake. The hazard takes the form of an overpowering rolling moment on the encountering aircraft. The magnitude of the overturning moment is crucial in the determination of safe aircraft spacing during landing and takeoff. Since a number of situations are potentially hazardous, the NASA effort has concentrated on possible ways to reduce the induced rolling moment on the encountering aircraft to a controllable level. A large part of the experimental program at Ames Research Center is being carried out in the 40- by 80-Foot Wind Tunnel. As part of this investigation, the wakes of several different wings and aircraft were studied to determine the vortex structure and the rolling moments induced on the following aircraft. Various methods for alleviating the rolling-moment hazard such as turbulence injection (refs. 1-3) and span-load modification (refs. 4-6) have also been studied by NASA and the excitation of vortex instabilities (ref. 7) has been studied at MIT under NASA sponsorship.

The investigation reported here is part of the foregoing general study on the magnitude of the wake-vortex hazard. Two wind-tunnel models were used to generate the vortex wake. One of them was typical of subsonic transports and the other of supersonic transports. Three different following models were used. The experiments were conducted in the test section of the NASA-Ames Research Center 40- by 80-Foot Wind Tunnel. The rolling moment measurements were made using a technique similar to that used by Wentz, Singh, Banta, Iversen, and Dunham (refs. 8-12, respectively). The work of Dunham (carried out concurrently) uses an identical aircraft model for the follower and subsonic generator. His test differs in that the models are towed through water

rather than air and his results extend to greater distances aft of the wake-generating model. Although lift on the generator was not varied by Dunham, duplicate conditions were tested so that the two results for the subsonic-transport models could be compared.

APPARATUS AND TEST PROCEDURE

Wind Tunnel Setup

A schematic diagram of the experimental setup is shown in figure 1 with the subsonic generator model at the forward end of the test section and the following model at the exit of the test section of the NASA-Ames Research Center 40- by 80-Foot Wind Tunnel. The generator model is centrally located in the inlet and is attached to a single strut through a strain gage balance to measure lift. The angle of attack of the generator was set remotely through an actuator and indicator. Downstream of the generator model 24.4 m (80 ft) a follower model was mounted on a single strut that could be remotely positioned vertically over a 3.05 m (10 ft) range and laterally over a 4.27 m (14 ft) range. The downstream distance of the follower model is varied by moving the entire tower assembly forward or aft in the test section. Additional details of the follower models are given in table I. It was attached to its strut through a strain gage balance to measure rolling moment. Full-scale range for this balance was 11.3 Nm (100 in.-lb) which provided adequate sensitivity for the rolling moments encountered when the free-stream velocity was about 40 m/sec ($q = 20 \text{ lb/ft}^2$). The following models were constructed of balsa wood to insure a high frequency response. The natural frequency of the model-balance combination (31 Hz, model 1) was several times larger than the rolling-moment frequencies encountered. The subsonic transport model (fig. 2) was equipped with two spanwise segments of trailing edge flaps capable of producing high lift. Full-span leading-edge flaps were installed with the high lift (or landing) configuration. The supersonic transport model was tested at various angles of attack in only the one configuration shown in figure 2(b) with no flaps deflected (which is the standard landing and takeoff configuration).

Photographs, presented in figure 3, of the two generating models mounted in the wind-tunnel test section show the general test arrangement. A rake located ahead of the SST model shown in figure 3(b) is used to produce a sheet of smoke for flow visualization. The rake and its support structure are removed before rolling-moment measurements are made.

Rolling-Moment Measurement

The procedure for recording the rolling moment consisted of setting the generator model and wind-tunnel conditions and selecting a lateral and vertical position for the following model. The time-varying rolling-moment signal was recorded on a light beam strip chart recorder. Sufficient length of record was taken to obtain the highest or peak rolling moment for that location (usually about one minute). The procedure was then repeated at successive lateral and vertical positions of the aft model in about 10 cm (4 in.) increments to determine the maximum value of rolling moment for each condition. Figure 4 shows a

typical record of rolling moment variation with time. It should be noted that during the 38 seconds of data shown, the peak rolling moment was repeated 3 times.

Measurements made of the rolling moment induced on several following models by the wake of both the subsonic- and supersonic-transport models were reduced to a rolling-moment coefficient defined as

$$C_{L_f} = \text{torque} / \left(\frac{1}{2} \rho U_\infty^2 b_f S_f \right)$$

where ρ is the air density, U_∞ the free-stream velocity, and b_f and S_f are, respectively, the span and wing area of the following model. The lift on the model used to generate the vortex wake is also presented in dimensionless form as

$$C_{L_g} = \text{lift} / \left(\frac{1}{2} \rho U_\infty^2 S_g \right)$$

where S_g is the wing area of the generating model.

DISCUSSION OF RESULTS

Rolling Moment

As mentioned in the foregoing section of the paper and illustrated in figure 4, the only values of torque which are retained are the maximum or peak values for a particular test configuration. Since the magnitude of these peak values changes with location of the follower model in the wake, a survey was first made of the peak torque as a function of vertical and lateral distance across the wake. A graph of the contours of equal rolling-moment coefficient is shown for both generating models in figures 5(a) and 5(b). The contours for the two models appear much the same except that the SST curves are broadened in the horizontal rather than the vertical direction. Both wakes have irregularities attributable to eddies in the wind-tunnel air stream and the manner in which the data are taken.

The maximum values found by such surveys over the entire wake for the various follower/generator combinations are shown in figure 6(a) as a function of lift on the wake-generator models, C_{L_g} . The SST model was tested at angles of attack of 9° , 12° , and 15° and the subsonic transport model at 2° to 14° in 2° increments (which covers the angle-of-attack range used for landing for both aircraft). It should first be noted that the rolling moment on the following model increases nearly linearly with C_{L_g} up to the beginning of flow separation of the generator model. This result is expected because the shape of the span-load distribution is nearly independent of C_{L_g} and only the magnitude of the lift changes with angle of attack. Since the vortex structure depends directly on the span loading (ref. 4), only the vortex strength changes with C_{L_g} thereby yielding the nearly linear relationship with C_{L_f} . It is also

interesting to observe in figure 6(a) that the three curves for the subsonic-transport model lie on approximately the same line. Also, the SST and subsonic transport when at their respective landing lift coefficients are noted to cause about the same rolling moment on the following model.

The span of the follower models tested differs for the two generators because their size relative to the full-sized counterparts are different. That is, the subsonic-transport model was about 3 percent of a full-scale, jumbo jet and the SST model was about 6 percent of a full scale version. The data points shown in figure 6(a) for the SST generator represent both follower models tested; i.e., $b_f/b_g = 0.61$ and 1.06 . The torque changed with span of the follower so that the rolling-moment coefficient was nearly the same for the two tests. A similar result was found for the subsonic transport although the follower with the smaller span yielded a slightly larger rolling-moment coefficient. Such a variation is expected for vortices with core diameters only moderately smaller than the model span. When the span of the follower is much larger than the core diameter of the vortex, the rolling-moment coefficient becomes independent of the vortex core structure and dependent only on the total circulation, Γ , in the vortex. Figure 6(b) confirms this observation by showing that the rolling-moment coefficients for all the models tested correlate quite well along a straight line for both generating models when plotted as a function of the dimensionless circulation in the wake vortices. The circulation parameter for figure 6(b) was estimated by assuming that the span loadings were approximately elliptical so that

$$\Gamma/bU_\infty = 2C_{L_g} / (\pi R_g)$$

where R_g is the aspect ratio of the wake-generating wing.

The data in figure 6 do not show a dependence of rolling moment on downstream distance. An estimate of whether decay should have occurred in the 24 m test distance behind the generating models can be made using the vortex correlation of Ciffone (ref. 13). The maximum rotational velocities in the vortex are first estimated from hot-wire data to be less than about $0.5 U_\infty$. For this value the beginning of decay for the vortices is then determined from the data correlation of Ciffone (ref. 13) to occur at 15 to 20 spans behind the generating wing. It is concluded therefore that the measurements were made largely in the so-called "plateau region" identified by Ciffone and Orloff (ref. 6) rather than in the decay region. A substantial change in torque on a following model as distance behind the generator model increases is therefore not to be expected for these tests. Since no data was taken at larger downstream distances where the vortices would be decaying, no conclusions are drawn as to the rate of decrease in rolling moment with greater downstream distances.

Smoke-Flow Visualization

Smoke (oil mist) was dispensed ahead of both wake-generating models to obtain a qualitative picture of the vortex wakes. These wakes were viewed when illuminated by the lights of the wind tunnel and with focussed light slits from projectors. In general, the wakes of the two generators was about the same in that both displayed the classical wake pattern of two oppositely rotating

vortices (one pair) which were easily identified in the wake. As the lift coefficient increased, the general nature of the pattern was unchanged except that the midspan position of the wake was deflected downward a greater distance, reflecting the increased circulation and greater downwash. From these observations, it was noted that the wake of the SST model was larger than that of the subsonic transport model. Also the phenomenon often referred to as vortex bursting was not observed in any of the flow visualization studies with either model. A bursting of a vortex from near the apex of the delta wing on the SST might have occurred and not been detected because of the way the smoke from the rake flowed over the wing. However, the wind-tunnel data of Wentz and Kohlman (ref. 14) indicate that bursting of any leading-edge vortex that may be present might require a larger angle of attack than was used during these tests of the SST model.

CONCLUDING REMARKS

The measurements made in the wake of a subsonic- and a supersonic-transport model indicate rolling-moment coefficients that increase approximately linearly over the angle-of-attack range wherein negligible flow separation occurs. Flow visualization indicated only one vortex pair behind both models and no vortex instabilities or core bursting were observed within the downstream distances tested. Although the rolling-moment coefficients for the two models varied appreciably, they had about the same value at the landing attitude of the full-scale or flight configurations. Furthermore, the rolling-moment coefficient for various following models behind both wake-generating models could be correlated on a straight line when plotted as a function of the dimensionless vortex strength.

The data taken in the wind-tunnel scales to about 0.85 and 0.42 km (1/2 and 1/4 mile), respectively, behind the full-scale versions of subsonic- and supersonic-transport. Although these results are indicative of the magnitude to be expected, the nature of the vortex wakes and the rolling moments induced on encountering aircraft needs to be investigated at the more practical spacing of aircraft in the 3-8 km (2-5 miles) separation range.

REFERENCES

1. Patterson, J. C. Jr.: Lift-Induced Wing-Tip Vortex Attenuation. AIAA Paper No. 74-38, AIAA 12th Aerospace Sciences Meeting, Washington, D.C., Jan. 1974.
2. Corsiglia, V. R.; Jacobsen, R. A.; and Chigier, N.: An Experimental Investigation of Trailing Vortices Behind a Wing With a Vortex Dissipator. Aircraft Wake Turbulence, Edited by John H. Olsen, Arnold Goldberg and Milton Rogers, Plenum Publishing Corp., New York, Sept. 1970.
3. Corsiglia, V. R.; Schwind, R. K.; and Chigier, N. A.: Rapid-Scanning, Three-Dimensional Hot-Wire Anemometer Surveys of Wing-Tip Vortices. AIAA J. Aircraft, vol. 10, no. 12, Dec. 1973, pp. 752-757.
4. Rossow, V. J.: On the Inviscid Rolled-Up Structure of Lift-Generated Vortices. AIAA J. Aircraft, vol. 10, no. 11, Nov. 1973, pp. 647-650.
5. Rossow, V. J.: Theoretical Study of Lift-Generated Vortex Sheets Designed to Avoid Rollup. NASA TM X-62,304, Sept. 1973.
6. Ciffone, D. L.; and Orloff, K. L.: Far Field Wake Vortex Characteristics of Wings. AIAA 7th Fluid and Plasma Dynamics Conference, Palo Alto, Calif., June 17-19, 1974.
7. Bilanin, A. J.; and Widnall, S. E.: Aircraft Wake Dissipation by Sinusoidal Instability and Vortex Breakdown. AIAA Paper 73-107, Washington, D.C. 1973.
8. Wentz, W. H. Jr.: Evaluation of Several Vortex Dissipators by Wind Tunnel Measurements of Vortex-Induced Upset Loads. Wichita State Univ. Aeronautical Report 72-3, Sept. 1972.
9. Singh, B.; Kutty, T. M.; and Wentz, W. H. Jr.: Preliminary Investigation of Rolling Moments Induced by Trailing Vortices for Several Wing-Tip Modifications, Wichita State Univ. Aeronautical Report 72-1, Jan. 1972.
10. Banta, A. J.: Effects of Planform and Mass Injection on Rolling Moments Induced by Trailing Vortices. Master's Thesis, Wichita State University, Wichita, Kansas, Dec. 1973.
11. Iversen, J. D.; and Bernstein, S.: Trailing Vortex Effects on Following Aircraft, AIAA J. Aircraft, vol. 11, no. 1, Jan. 1974, pp. 60-61.
12. Dunham, E. R. Jr.: Model Tests of Various Vortex Dissipation Techniques in a Water Towing Tank. Prospective NASA Tech. Note.
13. Ciffone, D. L.: Correlation for Estimating Vortex Rotational Velocity Downstream Dependence. AIAA J. Aircraft, vol. 11, no. 11, Nov. 1974, pp. 716-717.
14. Wentz, W. H., Jr.; and Kohlman, D. L.: Wind Tunnel Investigations of Vortex Breakdown on Slender Sharp-Edged Wings. Rept. FRL 68-013, Engineering Sciences Div., Univ. of Kansas Center for Research, Inc., Nov. 1968.

TABLE 1.- GEOMETRIC DETAILS OF FOLLOWING MODELS;
DIMENSIONS IN CM (IN.)

	Model number		
	1	2	3
Span	87.4 (34.4)	33.3 (13.1)	151.6 (59.8)
Aspect ratio	8.9	5.5	15.5
Wing section	NACA 0012		
Fuselage diameter	5.1 (2.0)		

REPRODUCIBILITY OF THE ORIGINAL PAGE IS POOR

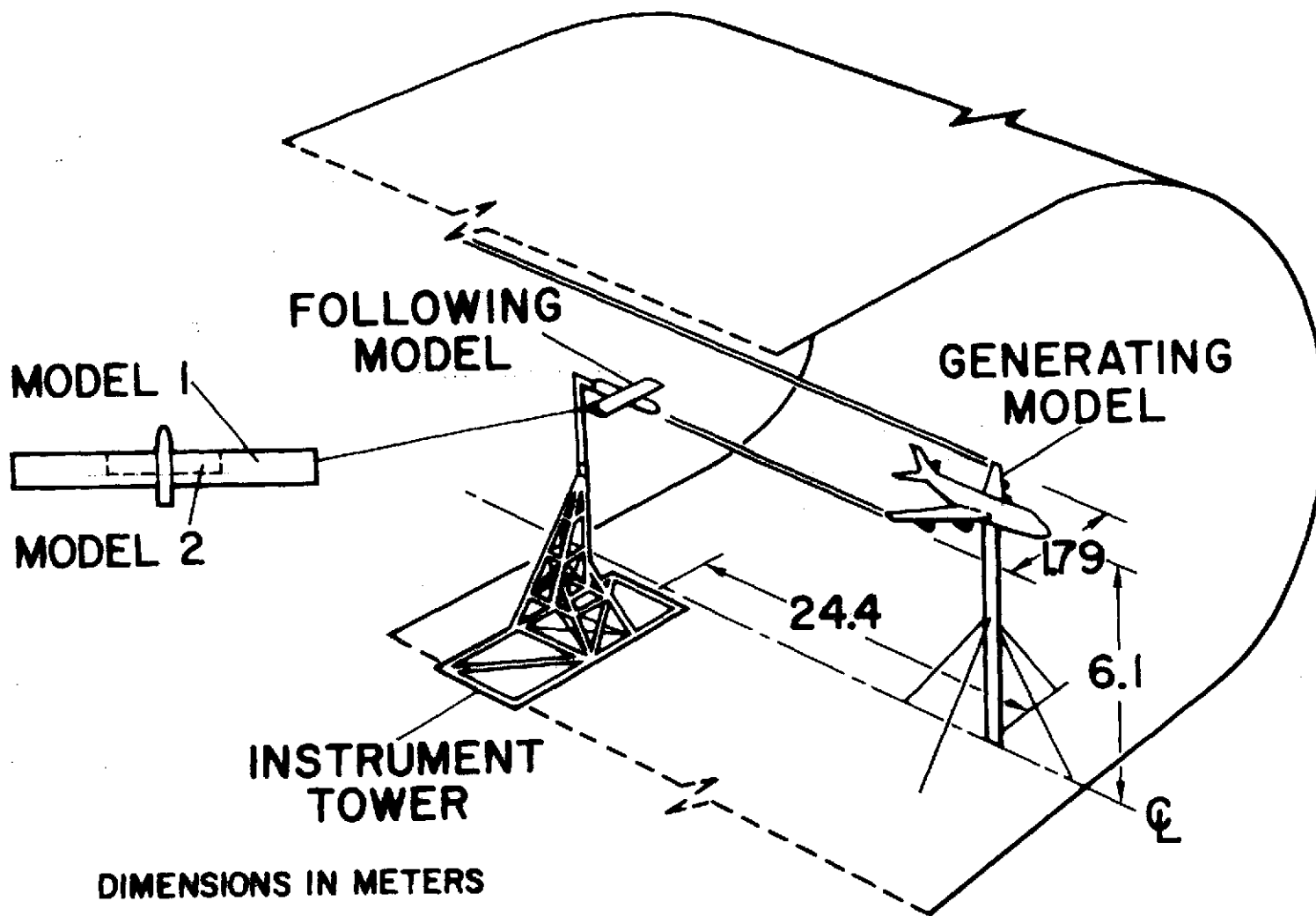
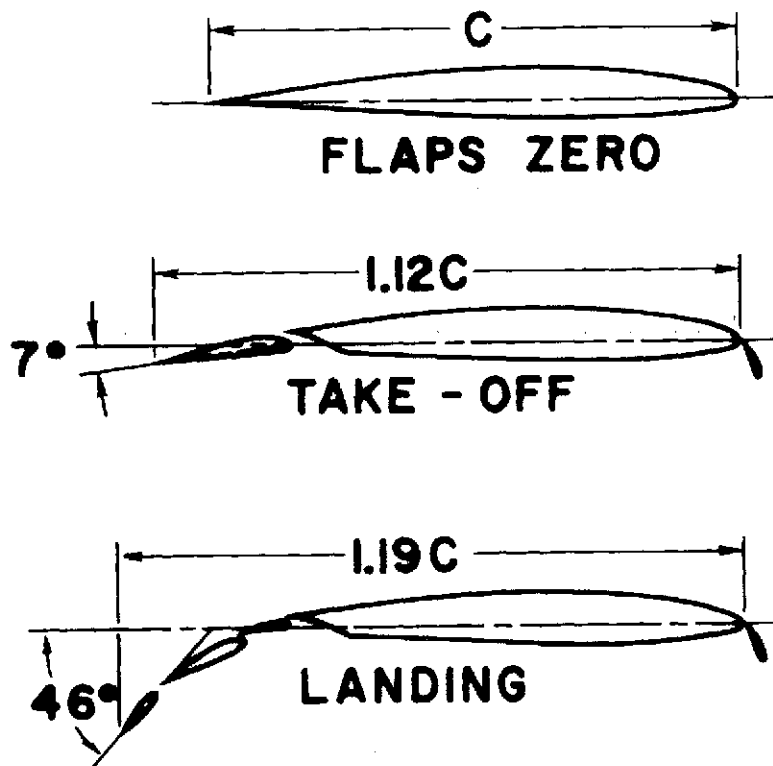
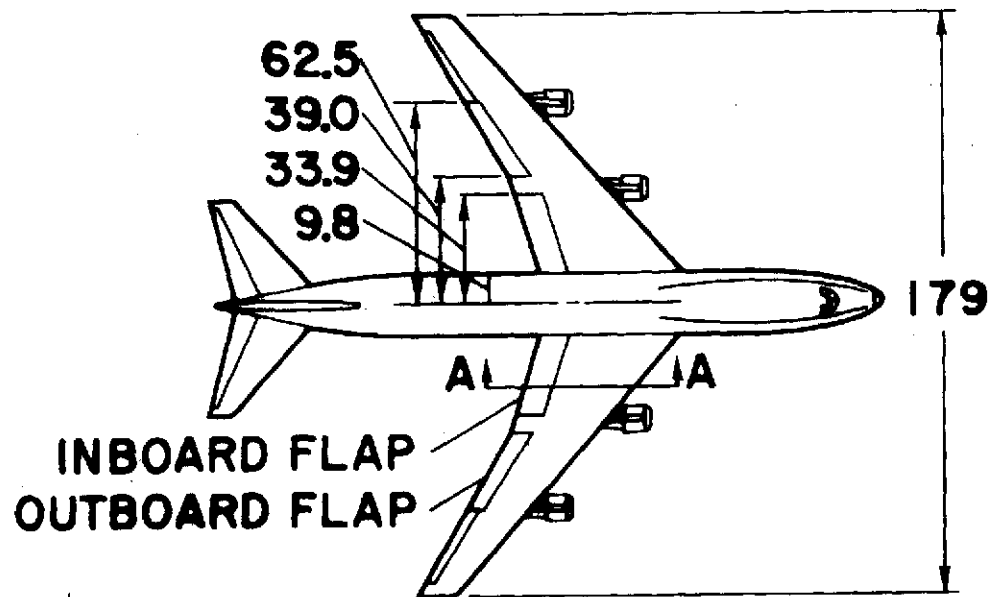


Figure 1.- Experimental setup in NASA Ames 40- by 80-Foot Wind Tunnel for measuring rolling moment on model in wake; dimensions given in meters.



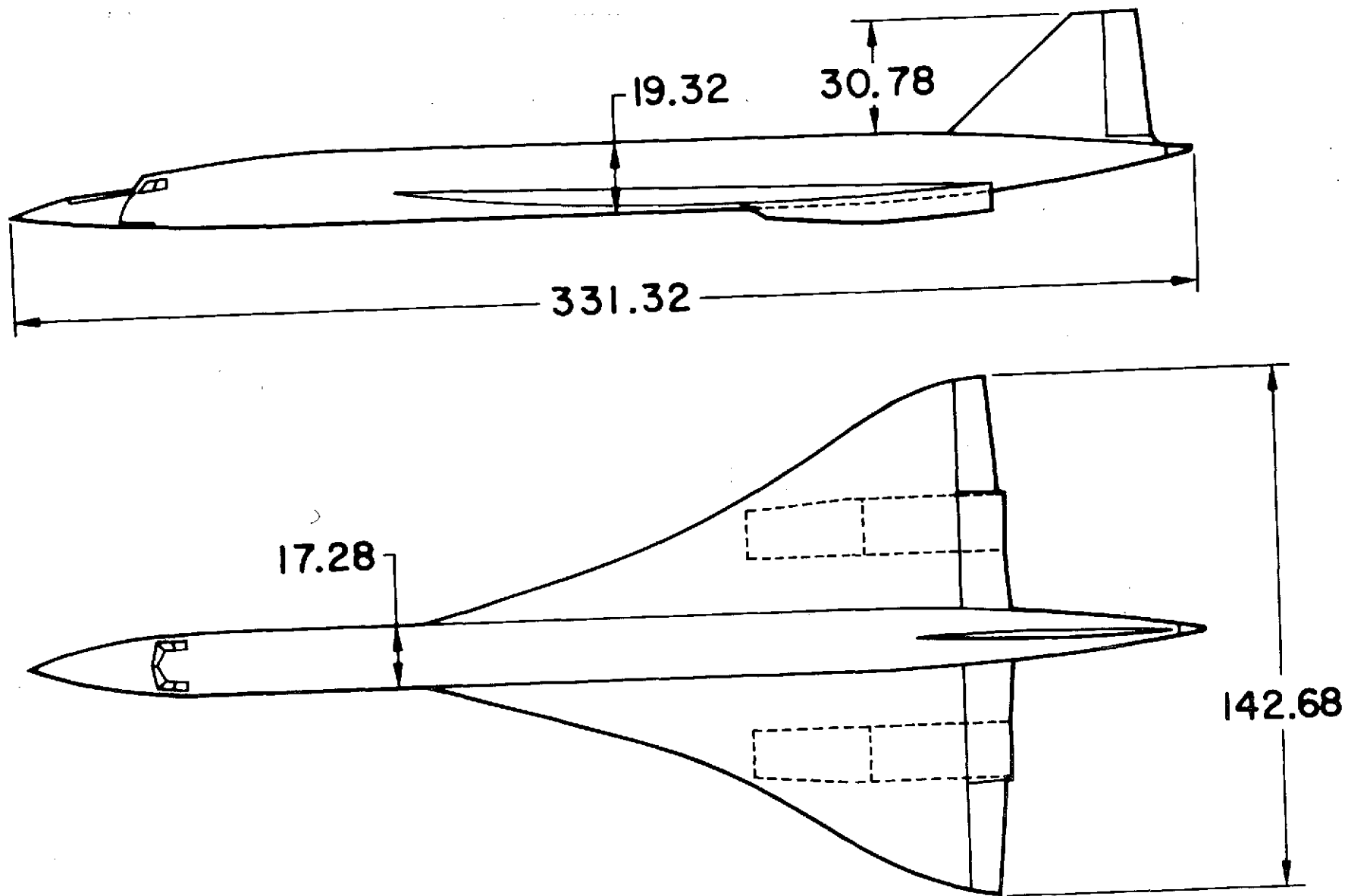
SECTION A-A DETAILS



DIMENSIONS IN cm

(a) Subsonic-transport model; about 3 percent of full scale.

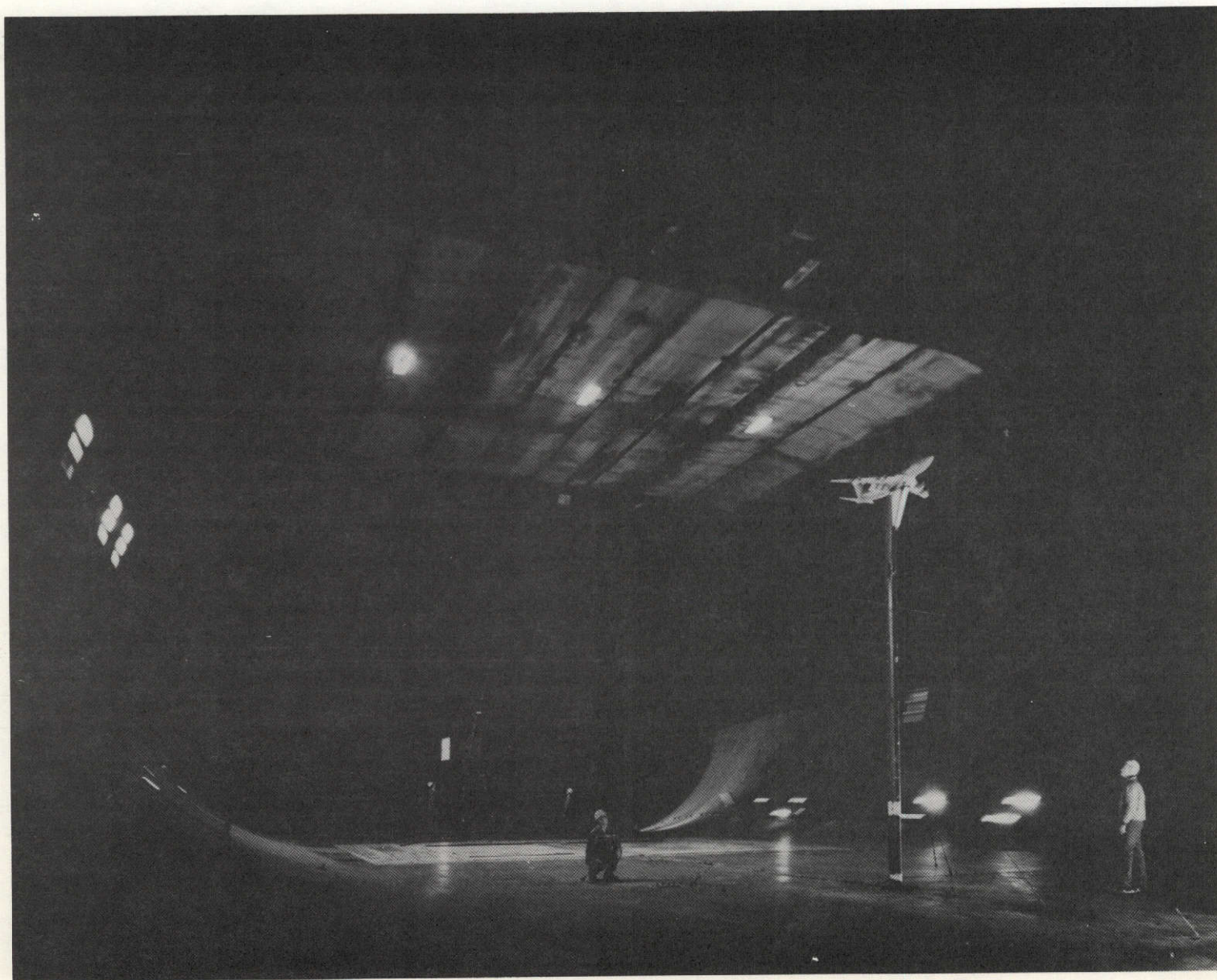
Figure 2.- Geometric details of models used to generate wake; dimensions given in cm.



(b) Supersonic-transport model; about 6 percent of full scale.

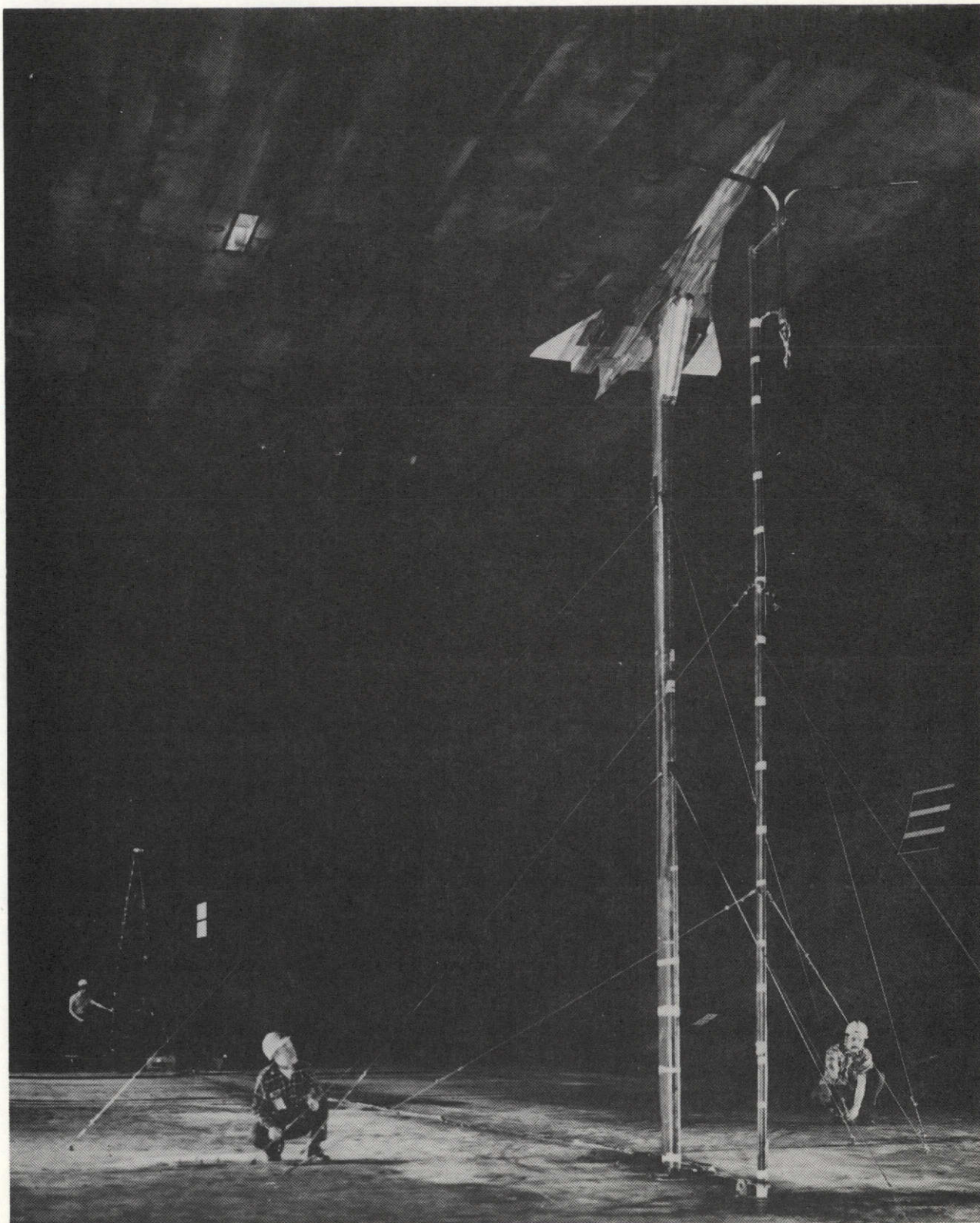
Figure 2.- Concluded.

REPRODUCIBILITY OF THE
ORIGINAL, PAGE IS POOR



(a) Subsonic-transport model.

Figure 3.- Photograph of setup in 40- by 80-foot wind tunnel.



(b) Supersonic-transport model.

Figure 3.- Concluded.

REPRODUCIBILITY OF THE
ORIGINAL PAGE IS POOR

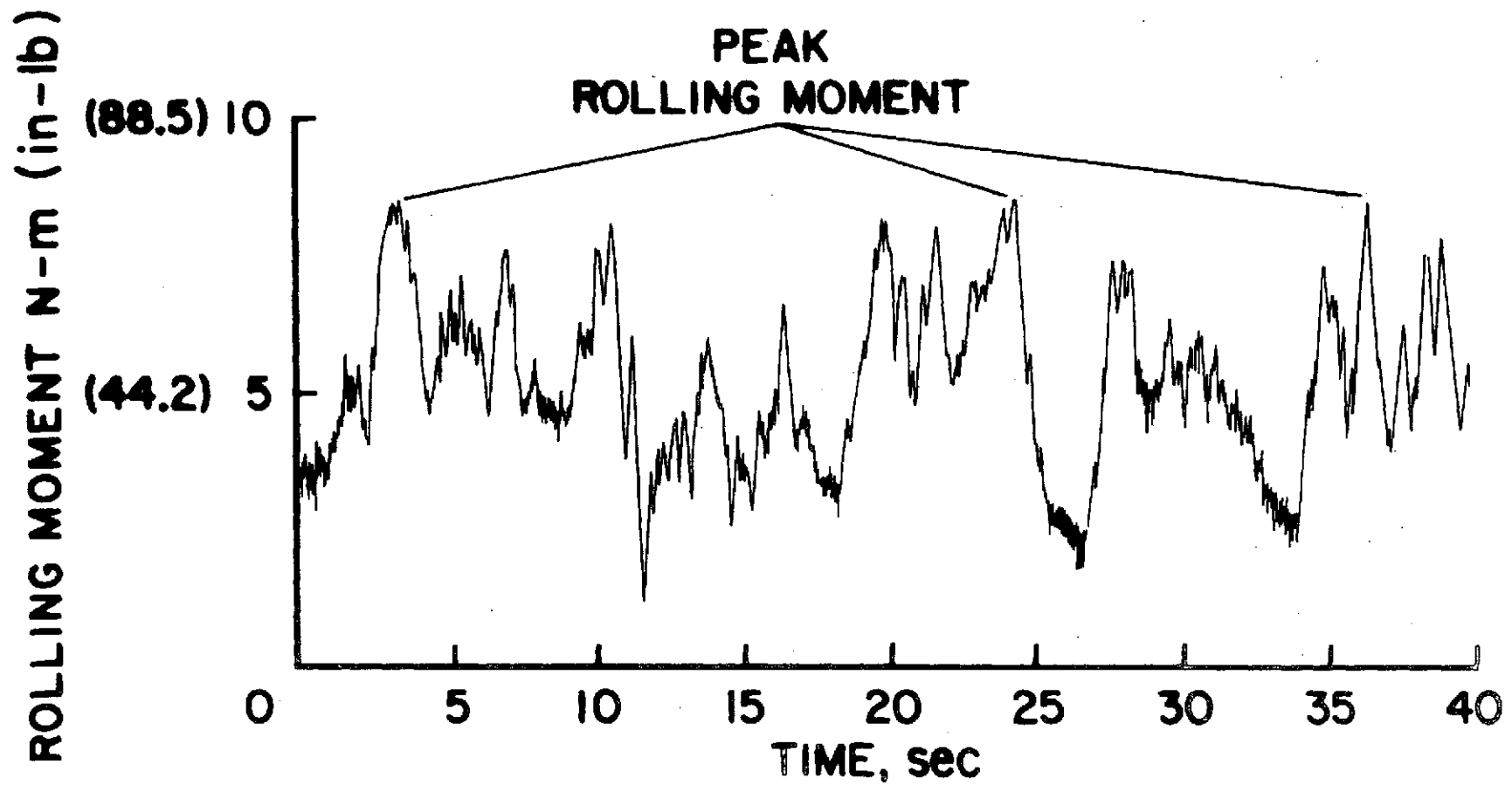
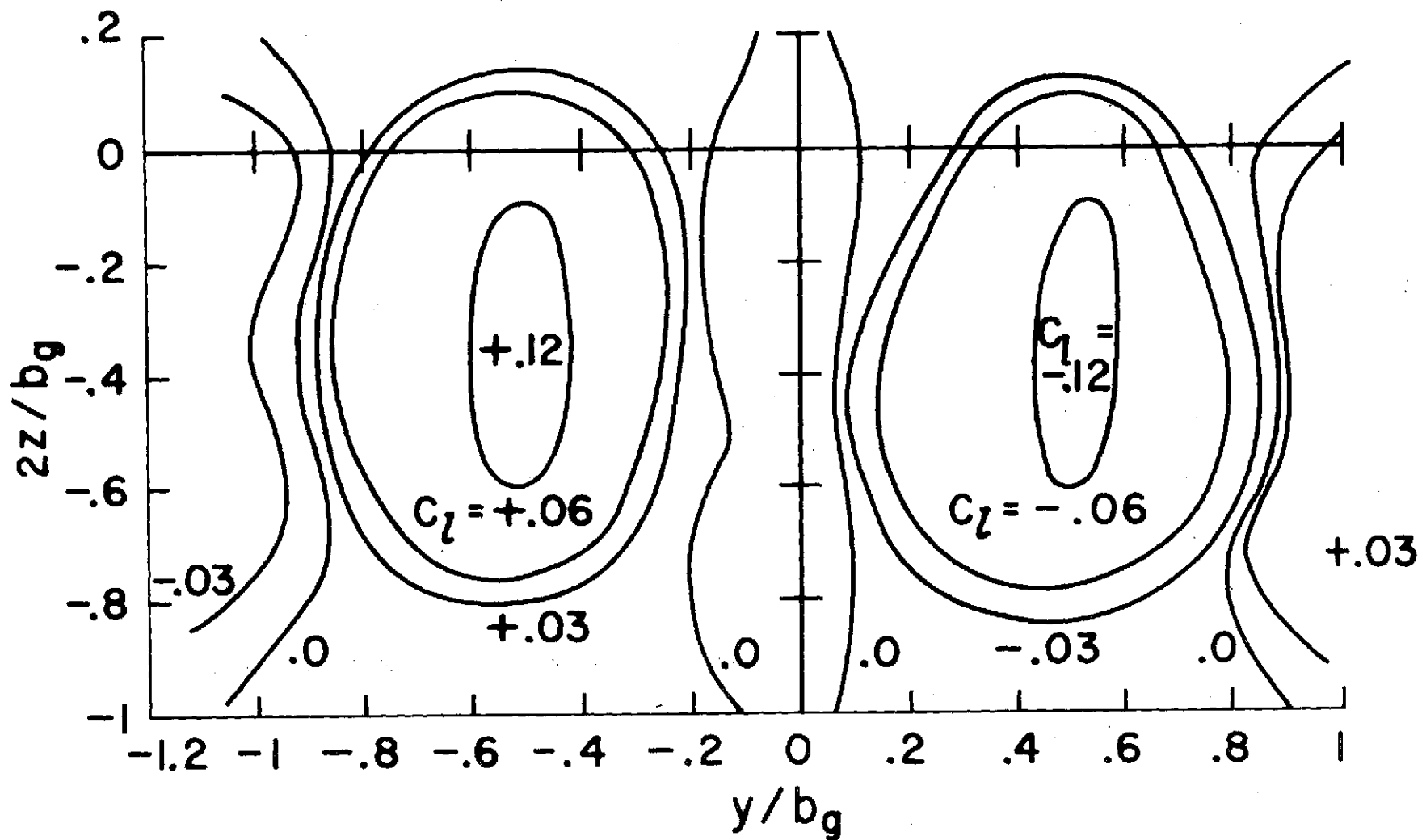
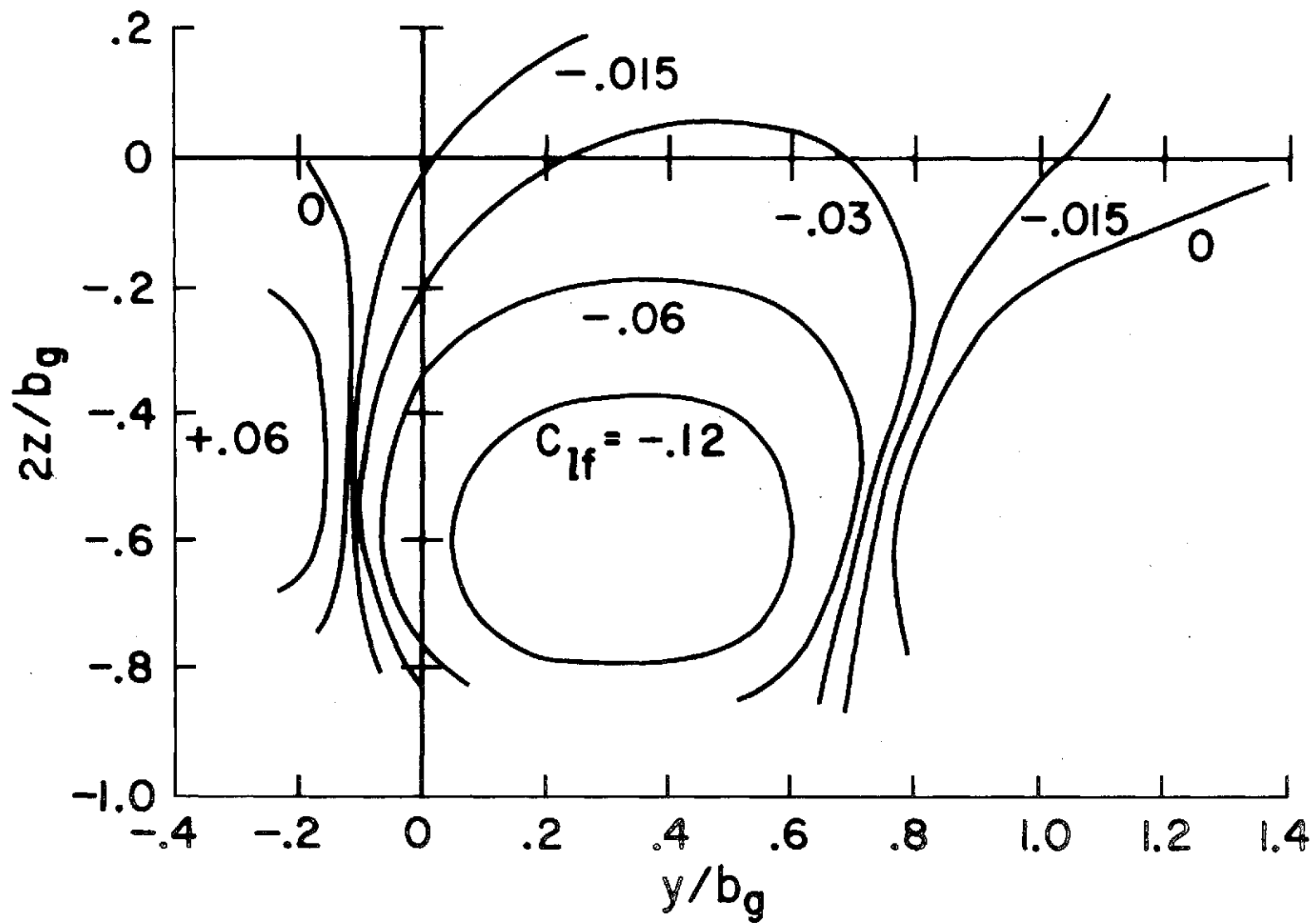


Figure 4.- Typical time-dependent record of rolling moment induced on following model #1 by subsonic-transport model in landing configuration.



(a) Subsonic-transport model.

Figure 5.- Contours of equal rolling-moment coefficient induced on following model #1 by the wake-generating models.



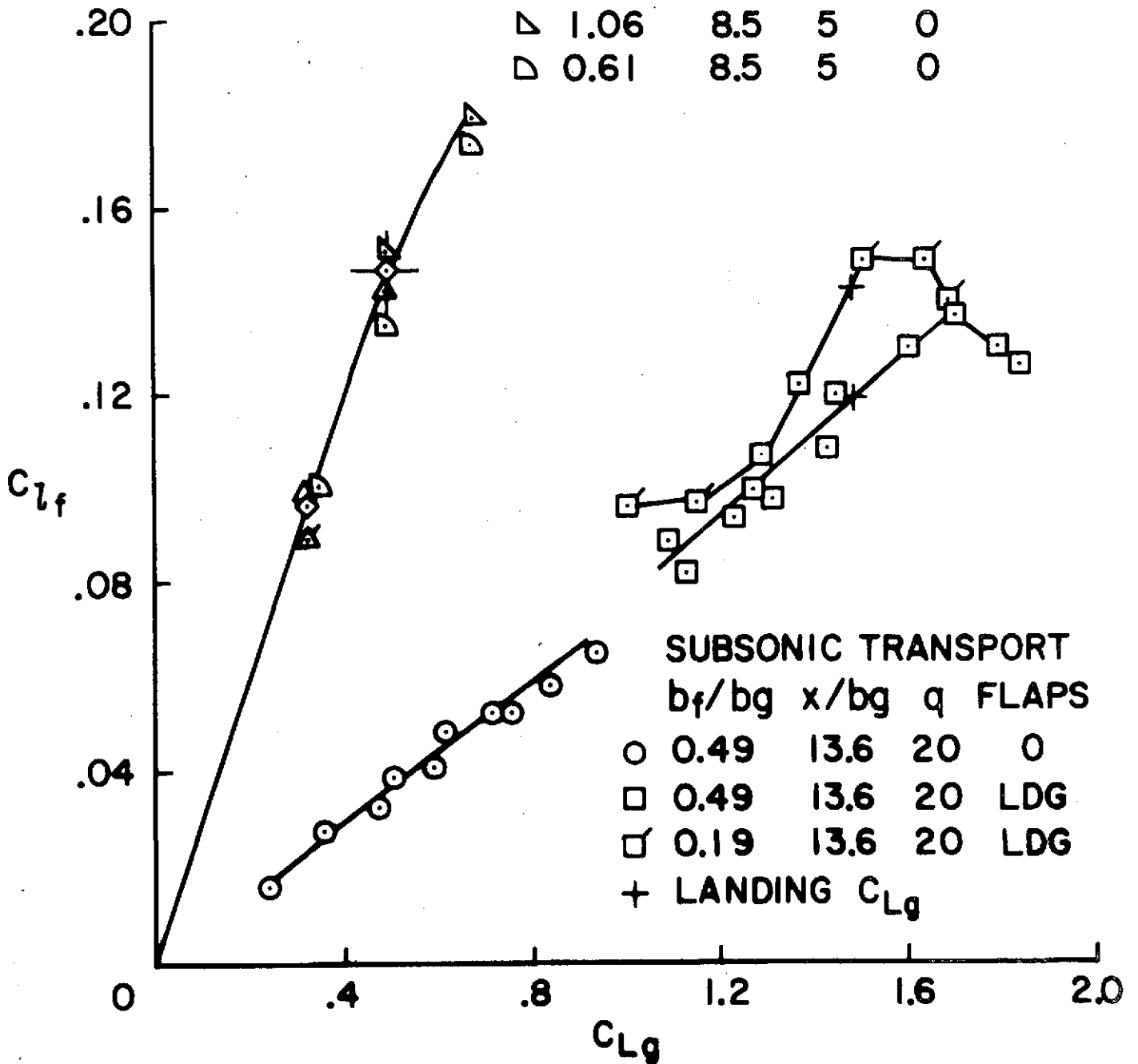
(b) Supersonic-transport model.

Figure 5.- Concluded.

SUPERSONIC TRANSPORT

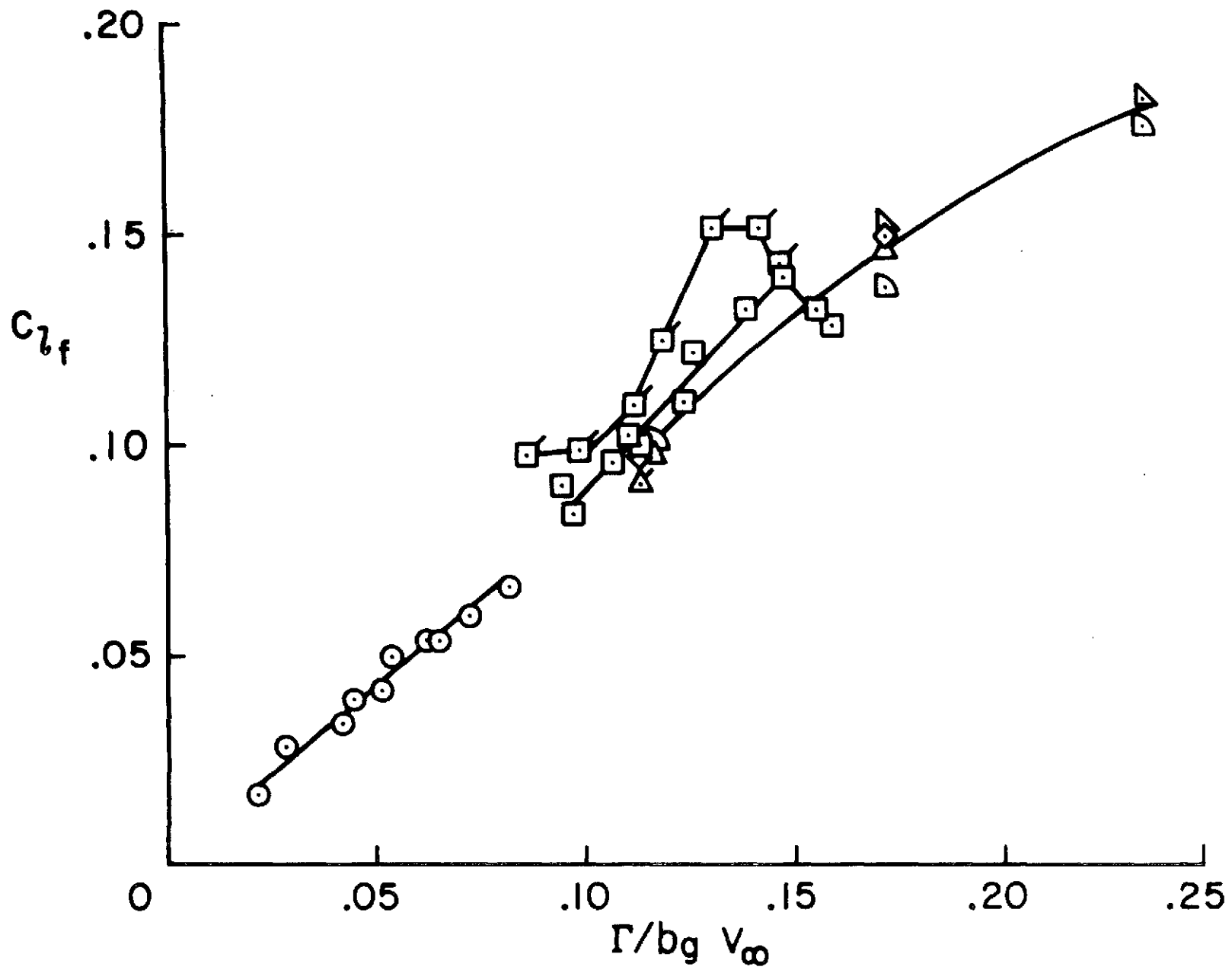
b_f/b_g x/b_g q FLAPS

◇	0.61	17	20	0
△	1.06	17	10	0
△	1.06	17	5	0
▷	1.06	8.5	5	0
▷	0.61	8.5	5	0



(a) As a function of lift on the generating model.

Figure 6.- Variation of peak rolling moment on following models.



(b) As a function of circulation in the lift-generated vortex.